Current Biology

Evolutionary History, Genomic Adaptation to Toxic Diet, and Extinction of the Carolina Parakeet

Highlights

- First whole genome from the extinct Carolina parakeet and the sun parakeet

- Divergence time between *Conuropsis* and *Aratinga* around 3 mya

- Evidence for potential adaptation to toxic diet in two extremely conserved proteins

- No signs of inbreeding in the Carolina parakeet suggest the extinction was abrupt

Authors

Pere Gelabert,
Marcela Sandoval-Velasco,
Aitor Serres, ..., Agostinho Antunes,
M. Thomas P. Gilbert,
Carles Lalueza-Fox

Correspondence

tgilbert@bio.ku.dk (M.T.P.G.),
carles.lalueza@upf.edu (C.L.-F.)

In Brief

Gelabert et al. report the whole genome of the extinct Carolina parakeet and provide evidence of its phylogeny, adaptation to a toxic cocklebur diet, and demographic history. The lack of signs of recent inbreeding typically found in endangered species suggests its abrupt extinction was human mediated.

CellPress

Cell**Press**

Evolutionary History, Genomic Adaptation to Toxic Diet, and Extinction of the Carolina Parakeet

Pere Gelabert,[1,2] Marcela Sandoval-Velasco,[3] Aitor Serres,[1] Marc de Manuel,[1] Pere Renom,[1] Ashot Margaryan,[3] Josefin Stiller,[4] Toni de-Dios,[1] Qi Fang,[5] Shaohong Feng,[5] Santi Mañosa,[6] George Pacheco,[3] Manuel Ferrando-Bernal,[1] Guolin Shi,[7] Fei Hao,[7] Xianqing Chen,[8] Bent Petersen,[3,9] Remi-André Olsen,[10] Arcadi Navarro,[1,11,12] Yuan Deng,[5] Love Dalén,[13] Tomàs Marquès-Bonet,[1,11,12,14] Guojie Zhang,[4,15,16,17] Agostinho Antunes,[18,19] M. Thomas P. Gilbert,[3,20,*] and Carles Lalueza-Fox[1,21,*]

[1]Institute of Evolutionary Biology (CSIC-Universitat Pompeu Fabra), Dr. Aiguader 88, 08003 Barcelona, Spain
[2]Department of Evolutionary Anthropology, University of Vienna, Althanstraße 14, 1090 Vienna, Austria
[3]Section for Evolutionary Genomics, The GLOBE Institute, University of Copenhagen, Øster Voldgade 5-7, 1350 Copenhagen, Denmark
[4]Section for Ecology and Evolution, Department of Biology, University of Copenhagen, Universitetsparken 15, 2100 Copenhagen, Denmark
[5]BGI-Shenzhen, Beishan Industrial Zone, Building 11, Shenzhen 518083, China
[6]Departament de Biologia Evolutiva, Ecologia i Ciències Ambientals, Institut de Recerca de la Biodiversitat (IRBio), Universitat de Barcelona, Facultat de Biologia, Avinguda Diagonal 643, 08028 Barcelona, Spain
[7]Center of Special Environmental Biomechanics & Biomedical Engineering, School of Life Sciences, Northwestern Polytechnical University, 127 West Youyi Road, Xi'an 710072, China
[8]Center for Ecological and Environmental Sciences, Northwestern Polytechnical University, 127 West Youyi Road, Xi'an 710072, China
[9]Centre of Excellence for Omics-Driven Computational Biodiscovery (COMBio), Faculty of Applied Sciences, AIMST University, Semeling Road, 08100 Kedah, Malaysia
[10]ScieLifeLab, Department of Biochemistry and Biophysics, Stockholm University, Frescativägen 40, SE-17121 Solna, Sweden
[11]Catalan Institution of Research and Advanced Studies (ICREA), Passeig de Lluís Companys 23, 08010 Barcelona, Spain
[12]CNAG-CRG, Centre for Genomic Regulation, Barcelona Institute of Science and Technology (BIST), Baldiri i Reixac 4, 08036 Barcelona, Spain
[13]Department of Bioinformatics and Genetics, Swedish Museum of Natural History, Frescativägen 40, 10405 Stockholm, Sweden
[14]Institut Català de Paleontologia Miquel Crusafont, Universitat Autònoma de Barcelona, c. de les Columnes s/n, 08193 Cerdanyola del Vallès, Barcelona, Spain
[15]China National GeneBank, BGI-Shenzhen, Jinsha Road, Shenzhen 518120, China
[16]State Key Laboratory of Genetic Resources and Evolution, Kunming Institute of Zoology, Chinese Academy of Sciences, 32 Jiaochang Donglu, Kunming 650223, China
[17]Center for Excellence in Animal Evolution and Genetics, Chinese Academy of Sciences, 32 Jiaochang Donglu, Kunming 650223, China
[18]CIIMAR/CIMAR, Interdisciplinary Centre of Marine and Environmental Research, University of Porto, Terminal de Cruzeiros do Porto de Leixões, Av. General Norton de Matos, s/n, 4450–208 Porto, Portugal
[19]Department of Biology, Faculty of Sciences, University of Porto, Rua do Campo Alegre s/n, 4169-007 Porto, Portugal
[20]NTNU University Museum, Erling Skakkes gate 47c, 7012 Trondheim, Norway
[21]Lead Contact
*Correspondence: tgilbert@bio.ku.dk (M.T.P.G.), carles.lalueza@upf.edu (C.L.-F.)
https://doi.org/10.1016/j.cub.2019.10.066

SUMMARY

As the only endemic neotropical parrot to have recently lived in the northern hemisphere, the Carolina parakeet (*Conuropsis carolinensis*) was an iconic North American bird. The last surviving specimen died in the Cincinnati Zoo in 1918 [1]. The cause of its extinction remains contentious: besides excessive mortality associated to habitat destruction and active hunting, their survival could have been negatively affected by its range having become increasingly patchy [2] or by the exposure to poultry pathogens [3, 4]. In addition, the Carolina parakeet showed a predilection for cockleburs, an herbaceous plant that contains a powerful toxin, carboxyatractyloside, or CAT [5], which did not seem to affect them but made the birds notoriously toxic to most predators [3]. To explore the demographic history of this bird, we generated the complete genomic sequence of a preserved specimen held in a private collection in Espinelves (Girona, Spain), as well as of a close extant relative, *Aratinga solstitialis*. We identified two non-synonymous genetic changes in two highly conserved proteins known to interact with CAT that could underlie a specific dietary adaptation to this toxin. Our genomic analyses did not reveal evidence of a dramatic past demographic decline in the Carolina parakeet; also, its genome did not exhibit the long runs of homozygosity that are signals of recent inbreeding and are typically found in endangered species. As such, our results suggest its extinction was an abrupt process and thus likely solely attributable to human causes.

RESULTS

The Carolina Parakeet and the Sun Parakeet Genomes

Given that *de novo* genome assembly is impractical with the typically short and degraded DNA found in historic and ancient
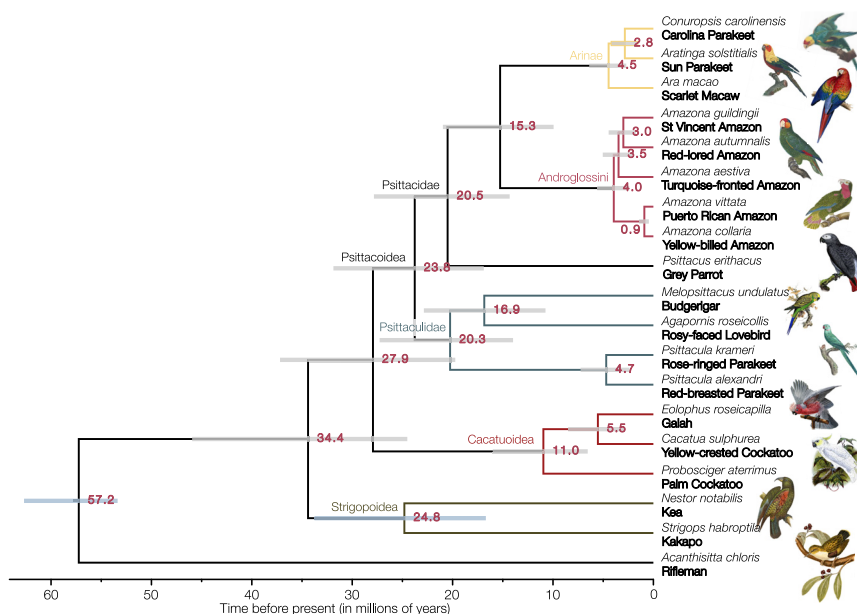
Figure 1. Phylogenetic Relationships of the Carolina Parakeet

Calibrated phylogeny built with BEAST2 based on 50 nuclear UCE loci from 18 species of parrots and a passerine (common names in bold). The analysis was constrained to a topology obtained from maximum likelihood analysis of 4,988 nuclear loci (9,864,148 bp), in which all nodes had 100 bootstrap support. Node ages were estimated using two fossil calibrations (highlighted in blue HPD intervals); gray bars indicate 95% HPD intervals of unconstrained nodes. Clade names follow a recent nomenclature revision [23]. See also Figure S2.

substitutions in all genes (dN/dS) is 0.48, and values similar to these have been reported in other bird genomes [15–17].

Sex determination of the specimens is difficult using morphological observations alone, as they have been described as being alike in coloration [4]. Females are the heterogametic sex (ZW) in birds; using genetic data, we were able to conclude that our specimen was a female because it showed about half the average depth coverage on the sex chromosomes (e.g., 13.4× genome-wide versus 7.11× at the DMRT1 gene that is located in the Z chromosome).

Phylogenetic Relationships

In order to investigate the phylogenetic placement of *Conuropsis* within Psittaciformes and estimate its divergence time, we used 4,988 nuclear loci (ultraconserved elements [UCEs], comprising 9,864,148 bp) extracted from the genomes of *C. carolinensis*, 17 extant parrots, and the rifleman *Acanthisitta chloris* (Passeriformes) as an outgroup. Individual gene trees summarized into a coalescent species tree were congruent with concatenated datasets and supported by maximum local posterior probability in all but one node. Gene trees suffered from the few and unusually short loci of one of the samples (*Strigops habroptila*; 77% of loci missing and 95.81% gaps across the concatenated alignment), which resulted in a low supported relationship with Psittacoidea (support = 0.23). This sample was also problematic in coalescent-based analyses in the original study that generated the data [18–21]. Concatenated analyses of all loci and of 95% and 100% completeness were congruent and had maximum bootstrap support for *Strigops+Nestor* as the sister to all other parrots, as found before [18–21]. All other relationships and the placement of *Conuropsis* were entirely congruent between analyses suppress unambiguous and highly supported. *Conuropsis* was consistently placed as the sister group of *Aratinga*, which in turn is sister group to the macaw *Ara* within Arinae (macaws, conures, and allies) (Figure 1). We also used the complete coding region of the mitochondrial (mtDNA) genome sequence to investigate the placement of *Conuropsis* against a greater sampling within the Arini and found the same placement as with nuclear data (Figure S2). Molecular clock analysis employing two fossil calibrations [21] suggests that the *Aratinga-Conuropsis* split occurred around 2.8 mya (1.6–
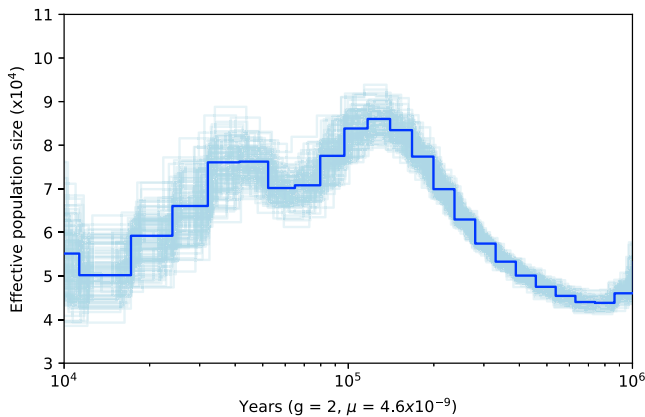
specimens [6, 7], we chose to generate a *de novo* assembly genome of the species' closest extant relative (*Aratinga solstitialis*; the sun parakeet), against which we could subsequently map and call full-genome variants from the sequenced Carolina parakeet (STAR Methods). Previous analyses of the phylogenetic relationship of the *Conuropsis* genus to extant parrots have been assessed based on morphology [8] and a short (876-nucleotide) fragment of the mtDNA genome retrieved from the toes of six specimens [9]. Both studies concluded that *Conuropsis* falls in a clade as a sister group to three *Aratinga* species [9]. Guided by this information, we generated a *de novo* reference genome of *Aratinga solstitialis* from a bird's breeder specimen. This genome was assembled and annotated using the B10K consortium pipelines [10] to render it consistent with previously published avian nuclear genomes during subsequent analyses. The genome was based on Illumina reads from three long-range Nextera libraries of different insert sizes and assembled with ALLPATH to a final N50 scaffold measure of 19.5 Mbp.

Following subsequent whole-genome shotgun sequencing of the Carolina parakeet DNA extract using the BGISeq-500 platform, which has been demonstrated to be effective for ancient DNA [11], we were able to map 209,887,920 unique reads from *C. carolinensis* against the 1,168,990,576 bp of *A. solstitialis* genome, covering 93% of the genomic positions, with a mean depth of 13.4× (STAR Methods). We also recovered the entire mtDNA genome to 150× depth of coverage. The reads exhibit characteristic ancient DNA deamination pattern at their ends [12], with a value close to 5% (Figure S1) that is consistent with our sample being just 100 years old [13]. We determined which positions were derived in *C. carolinensis* or *A. solstitialis* using the chicken *G. gallus* as outgroup. A total of 28,348 missense and 152 nonsense mutations were identified between *Conuropsis* and *Aratinga*. Of the former, 502 mutations were predicted to be deleterious mutations using SIFT software [14]. The Carolina parakeet transition/transversion (Ts/Tv) value is 2.309, the ratio of the non-synonymous to synonymous

Figure 2. Demographic History of the Carolina Parakeet

Pairwise sequentially Markovian coalescent (PSMC) plot shows *Conuropsis carolinensis* population history. We performed 100 bootstrap repetitions. The PSMC plot shows demographic fluctuations of the parakeet population size starting with the beginning of the Last Glacial Period.

See also Figure S3.

4.4; 95% highest posterior density [HPD] interval) from nuclear genome data and around 3.8 mya (2.73–5.05; 95% HPD interval) from mtDNA data. Both dates roughly coincide with the widely recognized date of 3 mya for the final closure of the Panama Isthmus [22]. It seems plausible, therefore, that the dispersal to North America occurred after the North and South American landmasses were continuous.

Demographic History

We used the pairwise sequentially Markovian coalescent (PSMC) algorithm [24] to evaluate the past demographic evolution of *Conuropsis* and *Aratinga* species. We found that the Carolina parakeet population experienced an increase in effective population size (N_e) during the Middle Pleistocene, followed by demographic fluctuations that started during the Last Glacial Period (~110 kya) and a subsequent population decline that continued until recent times (Figure 2). In contrast, the PSMC of the endangered *Aratinga solstitialis* shows a stronger and continuous population decline and a longer period of lower effective population size than *Conuropsis* (Figure S3).

We then profiled both the overall heterozygosity across the genome and the distribution of long runs of homozygosity (RoHs) (Figure S4). The former is a measure of overall genetic diversity, whereas RoHs arise when identical chromosomal fragments are inherited from a recent common ancestor. Thus, significantly reduced heterozygosity is typical of populations that have been small and isolated for long periods, although elevated levels of RoH are usually observed in inbred populations [25]. Both may therefore be typical of endangered species. We found that *Conuropsis* had a heterozygosity slightly below the average across bird genomes [10] but clearly does not appear to be an outlier (Figure 3) (the low level of heterozygosity of our *Aratinga* specimen could be influenced by the fact that it was an individual bred in captivity). In addition, 188 total RoHs were detected for *Conuropsis* (9 of them >1 Mb), although for *Aratinga*, the number is much higher (611 total RoHs; 85 >1
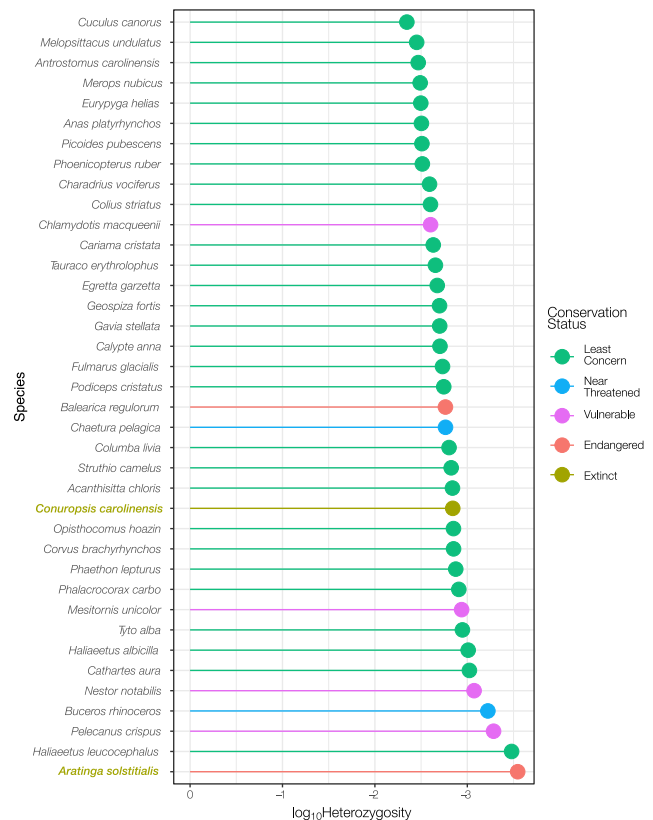

Figure 3. Genetic Diversity among Birds

Logarithm of the average genome heterozygosity for most published avian genomes. All species belong to different taxonomic orders except for *Conuropsis carolinensis* and *Aratinga solstitialis*, which are both Psittaciformes. Samples are colored by IUCN Conservation status.

See also Figure S4.

Mb) (Figure S4). Nevertheless, we report the presence of a single, long run of homozygosity of 7.15 Mb, which is suggestive of recent inbreeding in the ancestors of the Espinelves specimen. It cannot be discarded, in fact, that our specimen was originally bred in captivity. Alternatively, having only a single long RoH could be indicative of some selective sweep in that particular region.

Adaptation to Toxic Diet

We leveraged our data to explore the genomic basis of a curious behavior of this species, relating to its dietary habits. The Carolina parakeet consumed a variety of fruits, seeds, and to a lesser extent, buds and flowers, but most remarkably, it showed a predilection for cockleburs (*Xanthium strumarium*). This is unusual, as cockleburs contain significant levels of a diterpenoid glucoside, the carboxyatractyloside or CAT [5], a lethal toxin that inhibits mitochondrial energy production [26]. In a collection of 99 feeding observations of *Conuropsis*, the highest plant intake (n = 17) corresponded in fact to cockleburs [4]. CAT inhibits the function of four mitochondrial ATP transporters (ANT1, ANT2, ANT3, and ANT4; encoded by *SLC25A4*, *SLC25A5*, *SLC25A6*, and *SLC25A31*, respectively), which is lethal [26, 27]. We next explored these genes further by
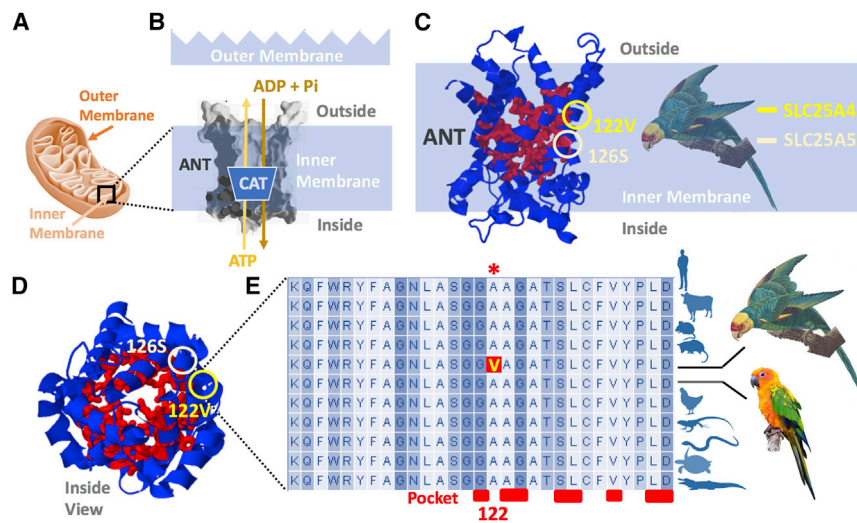
Figure 4. Adaptation to Toxic Diet

(A) Mitochondria representation of the outer and inner membrane (zoom in to B).

(B) Cartoon of the bovine ANT protein X-ray crystallographic structure (approximate location of the inhibition by CAT blocking the flux of ATP and ADP + Pi).

(C) Three-dimensional modeled structure of the SLC25A4 in *Conuropsis* with variable positions of the SLC25A4 in yellow and SLC25A5 in light orange (both modeled protein structures are quite similar—so only one was represented for simplification). The red region of the protein corresponds to the pocket.

(D) Inside view of the 3D modeled structure of the SLC25A4 in *Conuropsis* (positions labeled as in C).

(E) Sequential depiction of the amino acids around the position A122V of *SLC25A4* in *Conuropsis* (comparison bottom-down: human; cow; mouse; opossum; *C. carolinensis*; *A. solstitialis*; chicken; anoles; python; green turtle; and crocodile) and indication of the pocket sites (in red) in the protein segment represented.

comparing them against their orthologs in other available avian genomes, including one recently generated dataset representing 363 species spanning nearly all avian families [28]. First, we found that *SLC25A6* and *SLC25A31* genes are not present in that dataset, presumably due to the annotation pipeline used. We did, however, find that the *Conuropsis SLC25A4* and *SLC25A5* genes carry two non-synonymous amino acid changes with respect to the *Aratinga* annotation: A122V in *SLC25A4* (a C to T substitution covered by 14 DNA reads) and T126S in *SLC25A5* (an A to T substitution covered by 13 DNA reads). An additional variant in this gene, V227A, is shared with 24 other species from different orders. The two *SLC25A4* and *SLC25A5* substitutions found are conserved in a diverse dataset of vertebrates, in 37 previously published avian genomes [10], and in the newly available avian genome dataset (Figure 4). Among the large avian dataset, additional non-synonymous substitutions in the four codons preceding and opposite these two positions have only been found in one single species (*Pomatorhinus ruficollis*). The two sites are located in a helix of the protein and are flanking pocket sites, likely influencing the functionality of both proteins. Therefore, it is possible that these mutations conferred the species with a unique adaptive mechanism for dealing with the toxic CAT present in its diet, although we do not know whether they could be shared with other *Aratinga* species (besides *A. solstitialis*).

DISCUSSION

The extinct Carolina parakeet's genome could provide evidence for specific adaptive peculiarities of this species and also help answer questions related to the population history and extinction dynamics of this paradigmatic bird.

Taking advantage of having eighteen available parrot genomes, we have generated the first Psittaciformes genome-wide phylogeny, which showed that the divergence time for *Conuropsis* evolutionary lineage and its subsequent colonization of the North American subcontinent took place around 3 mya. Considering that the time to the most recent common ancestor

of all Psittaciformes is at least ten times larger (about 34.4 mya), we can conclude that the evolutionary history underlying the Carolina-parakeet-specific adaptations is a rather recent process within this order of birds.

We also uncovered evidence of a past population history of expansions and contractions with low effective population size but no dramatic signals of widespread, recent inbreeding that interestingly were discernable in *Aratinga*. This suggests that, despite the perception of high parakeet abundance based on observations of large and noisy flocks, this species had experienced population contractions that were likely associated to past climatic oscillations. However, scarce evidence of inbreeding indicates that it suffered a very quick extinction process that left no traces in the genomes of the last specimens. In fact, the bird's final extinction was likely accelerated by collectors and trappers when it became evident that it was extremely rare [8].

We found evidence that the Carolina parakeet was adapted to the cocklebur's toxin, but we caution that this feeding behavior is not exclusive of *Conuropsis*; parrots in general ingest fruits and seeds known to be toxic to other vertebrates [29]. It has been proposed that some species could neutralize them by consuming clay from river banks, which would have a toxin-absorbing function [30], although other physiological detoxification mechanisms cannot be discarded. Nevertheless, it would be interesting in the future to functionally test the two variants detected in the *SLC25A4* and *SLC25A5* genes using avian cell lines.

Other potential factors for *Conuropsis* extinction, such as the exposure to poultry pathogens, will likely require a metagenomic screening of at least several parakeet specimens; however, preliminary results from our sample do not show a significant presence of bird viruses.

The potential adaptation to the CAT toxin and the lack of evidence for a dramatic long-term decline and widespread inbreeding suggests that no additional factors contributed to the extinction process. Therefore, the abrupt disappearance of the Carolina parakeet seems to be directly attributable to human pressures.

STAR★METHODS

Detailed methods are provided in the online version of this paper and include the following:

- KEY RESOURCES TABLE
- LEAD CONTACT AND MATERIALS AVAILABILITY
- EXPERIMENTAL MODEL AND SUBJECT DETAILS
  - Conuropsis carolinensis specimen
  - Aratinga solstitialis specimen
- METHOD DETAILS
  - *Conuropsis* DNA extraction and sequencing
  - *Aratinga solstitialis* DNA extraction
  - *Aratinga solstitialis* sequencing and assembly
  - *Aratinga solstitialis* annotation
  - *Conuropsis carolinensis* mapping and variant calling
  - Sex determination
  - Ultraconserved Elements (UCE) phylogenetic tree
  - Mitochondrial phylogenetic tree
  - *Conuropsis* population history
  - *Conuropsis* average genome heterozygosity
  - *Conuropsis* Runs of Homozygosity (RoHs)
- QUANTIFICATION AND STATISTICAL ANALYSIS
- DATA AND CODE AVAILABILITY

SUPPLEMENTAL INFORMATION

Supplemental Information can be found online at https://doi.org/10.1016/j.cub.2019.10.066.

AUTHOR CONTRIBUTIONS

P.R., C.L.-F., and M.T.P.G. conceived the project. P.R., S.M., and C.L.-F. studied and sampled the specimens. M.S.-V., G.P., G.S., F.H., and X.C. performed experimental work. P.G., A.S., A.M., J.S., T.d.-D., Q.F., S.F., M.F.-B., B.P., A.N., Y.D., and L.D. undertook different computational analyses. M.P.T.G., C.L.-F., L.D., T.M.-B., and G.Z. coordinated different computational teams. A.A. performed the *in silico* protein analysis. J.S. and A.A. worked in visualization. P.G., M.P.T.G., and C.L.-F. wrote the manuscript with input from all coauthors.

REFERENCES

1. Elphick, C.S., Roberts, D.L., and Reed, J.M. (2010). Estimated dates of recent extinctions for North American and Hawaiian birds. Biol. Conserv. *143*, 617–624.

2. Burgio, K.R., Carlson, C.J., and Tingley, M.W. (2017). Lazarus ecology: Recovering the distribution and migratory patterns of the extinct Carolina parakeet. Ecol. Evol. *7*, 5467–5475.

3. Snyder, N.F.R. (2004). The Carolina Parakeet: Glimpses of a Vanished Bird (Princeton University Press).

4. Snyder, N.F.R., and Russel, K. (2002). Carolina parakeet (*Conuropsis carolinensis*), version 2.0. In The Birds of North America, A.F. Poole, and F.B. Gill, eds. (Cornell Lab of Ornithology).

5. Stuart, B.P., Cole, R.J., and Gosser, H.S. (1981). Cocklebur (*Xanthium strumarium*, L. var. *strumarium*) intoxication in swine: review and redefinition of the toxic principle. Vet. Pathol. *18*, 368–383.

6. Prüfer, K., Stenzel, U., Hofreiter, M., Pääbo, S., Kelso, J., and Green, R.E. (2010). Computational challenges in the analysis of ancient DNA. Genome Biol. *11*, R47.

7. Shapiro, B., and Hofreiter, M. (2014). A paleogenomic perspective on evolution and gene function: new insights from ancient DNA. Science *343*, 1236573.

8. Forshaw, J.M. (1989). Parrots of the World Third Edition (Lansdowne Editions).

9. Kirchman, J.J., Schirtzinger, E.E., and Wright, T.F. (2012). Phylogenetic relationships of the extinct Carolina Parakeet (*Conuropsis carolinensis*) inferred from DNA sequence data. Auk *129*, 197–204.

10. Zhang, G., Li, B., Li, C., Gilbert, M.T., Jarvis, E.D., and Wang, J.; Avian Genome Consortium (2014). Comparative genomic data of the Avian Phylogenomics Project. Gigascience *3*, 26.

11. Mak, S.S.T., Gopalakrishnan, S., Carøe, C., Geng, C., Liu, S., Sinding, M.S., Kuderna, L.F.K., Zhang, W., Fu, S., Vieira, F.G., et al. (2017). Comparative performance of the BGISEQ-500 vs Illumina HiSeq2500 sequencing platforms for palaeogenomic sequencing. Gigascience *6*, 1–13.

12. Briggs, A.W., Stenzel, U., Johnson, P.L.F., Green, R.E., Kelso, J., Prüfer, K., Meyer, M., Krause, J., Ronan, M.T., Lachmann, M., and Pääbo, S. (2007). Patterns of damage in genomic DNA sequences from a Neandertal. Proc. Natl. Acad. Sci. USA *104*, 14616–14621.

13. Sawyer, S., Krause, J., Guschanski, K., Savolainen, V., and Pääbo, S. (2012). Temporal patterns of nucleotide misincorporations and DNA fragmentation in ancient DNA. PLoS ONE *7*, e34131.

14. Sim, N.L., Kumar, P., Hu, J., Henikoff, S., Schneider, G., and Ng, P.C. (2012). SIFT web server: predicting effects of amino acid substitutions on proteins. Nucleic Acids Res. *40*, W452-7.

15. Jonker, R.M., Zhang, Q., Van Hooft, P., Loonen, M.J.J.E., Van der Jeugd, H.P., Crooijmans, R.P.M.A., Groenen, M.A.M., Prins, H.H.T., and Kraus, R.H.S. (2012). The development of a genome wide SNP set for the Barnacle goose *Branta leucopsis*. PLoS ONE *7*, e38412.

16. Kraus, R.H.S., Kerstens, H.H.D., Van Hooft, P., Crooijmans, R.P.M.A., Van Der Poel, J.J., Elmberg, J., Vignal, A., Huang, Y., Li, N., Prins, H.H.T., and

Groenen, M.A. (2011). Genome wide SNP discovery, analysis and evaluation in mallard (Anas platyrhynchos). BMC Genomics *12*, 150.

17. van Bers, N.E.M., van Oers, K., Kerstens, H.H.D., Dibbits, B.W., Crooijmans, R.P.M.A., Visser, M.E., and Groenen, M.A.M. (2010). Genome-wide SNP detection in the great tit *Parus major* using high throughput sequencing. Mol. Ecol. *19 (Suppl 1)*, 89–99.

18. de Kloet, R.S., and de Kloet, S.R. (2005). The evolution of the spindlin gene in birds: sequence analysis of an intron of the spindlin W and Z gene reveals four major divisions of the Psittaciformes. Mol. Phylogenet. Evol. *36*, 706–721.

19. Tokita, M., Kiyoshi, T., and Armstrong, K.N. (2007). Evolution of craniofacial novelty in parrots through developmental modularity and heterochrony. Evol. Dev. *9*, 590–601.

20. Wright, T.F., Schirtzinger, E.E., Matsumoto, T., Eberhard, J.R., Graves, G.R., Sanchez, J.J., Capelli, S., Müller, H., Scharpegge, J., Chambers, G.K., and Fleischer, R.C. (2008). A multilocus molecular phylogeny of the parrots (Psittaciformes): support for a Gondwanan origin during the cretaceous. Mol. Biol. Evol. *25*, 2141–2156.

21. Oliveros, C.H., Field, D.J., Ksepka, D.T., Barker, F.K., Aleixo, A., Andersen, M.J., Alström, P., Benz, B.W., Braun, E.L., Braun, M.J., et al. (2019). Earth history and the passerine superradiation. Proc. Natl. Acad. Sci. USA *116*, 7916–7925.

22. O'Dea, A., Lessios, H.A., Coates, A.G., Eytan, R.I., Restrepo-Moreno, S.A., Cione, A.L., Collins, L.S., de Queiroz, A., Farris, D.W., Norris, R.D., et al. (2016). Formation of the Isthmus of Panama. Sci. Adv. *2*, e1600883.

23. Joseph, L., Toon, A., Schirtzinger, E.E., Wright, T.F., and Schodde, R. (2012). A revised nomenclature and classification for family-group taxa of parrots (Psittaciformes). Zootaxa *3205*, 26–40.

24. Li, H., and Durbin, R. (2011). Inference of human population history from individual whole-genome sequences. Nature *475*, 493–496.

25. Prado-Martinez, J., Hernando-Herraez, I., Lorente-Galdos, B., Dabad, M., Ramirez, O., Baeza-Delgado, C., Morcillo-Suarez, C., Alkan, C., Hormozdiari, F., Raineri, E., et al. (2013). The genome sequencing of an albino Western lowland gorilla reveals inbreeding in the wild. BMC Genomics *14*, 363.

26. Pebay-Peyroula, E., Dahout-Gonzalez, C., Kahn, R., Trézéguet, V., Lauquin, G.J.M., and Brandolin, G. (2003). Structure of mitochondrial ADP/ATP carrier in complex with carboxyatractyloside. Nature *426*, 39–44.

27. Maldonado, E.N., DeHart, D.N., Patnaik, J., Klatt, S.C., Gooz, M.B., and Lemasters, J.J. (2016). ATP/ADP turnover and import of glycolytic ATP into mitochondria in cancer cells is independent of the adenine nucleotide translocator. J. Biol. Chem. *291*, 19642–19650.

28. China National GeneBank (2016). The Bird 10,000 Genomes (B10K) Project. https://b10k.genomics.cn/index.html.

29. Gilardi, J.D., and Toft, C.A. (2012). Parrots eat nutritious foods despite toxins. PLoS ONE *7*, e38293.

30. Gilardi, J.D., Duffey, S.S., Munn, C.A., and Tell, L.A. (1999). Biochemical functions of geophagy in parrots: detoxification of dietary toxins and cytoprotective effects. J. Chem. Ecol. *25*, 897–922.

31. van der Zwan, H., van der Westhuizen, F., Visser, C., and van der Sluis, R. (2018). Draft de novo genome sequence of *Agapornis roseicollis* for application in avian breeding. Anim. Biotechnol. *29*, 241–246.

32. Wirthlin, M., Lima, N.C.B., Guedes, R.L.M., Soares, A.E.R., Almeida, L.G.P., Cavaleiro, N.P., Loss de Morais, G., Chaves, A.V., Howard, J.T., Teixeira, M.M., et al. (2018). Parrot genomes and the evolution of heightened longevity and cognition. Curr. Biol. *28*, 4001–4008.e7.

33. Oleksyk, T.K., Pombert, J.F., Siu, D., Mazo-Vargas, A., Ramos, B., Guiblet, W., Afanador, Y., Ruiz-Rodriguez, C.T., Nickerson, M.L., Logue, D.M., et al. (2012). A locally funded Puerto Rican parrot (*Amazona vittata*) genome sequencing project increases avian data and advances young researcher education. Gigascience *1*, 14.

34. Seabury, C.M., Dowd, S.E., Seabury, P.M., Raudsepp, T., Brightsmith, D.J., Liboriussen, P., Halley, Y., Fisher, C.A., Owens, E., Viswanathan, G., and Tizard, I.R. (2013). A multi-platform draft de novo genome assembly and comparative analysis for the Scarlet Macaw (*Ara macao*). PLoS ONE *8*, e62415.

35. Gnerre, S., Maccallum, I., Przybylski, D., Ribeiro, F.J., Burton, J.N., Walker, B.J., Sharpe, T., Hall, G., Shea, T.P., Sykes, S., et al. (2011). High-quality draft assemblies of mammalian genomes from massively parallel sequence data. Proc. Natl. Acad. Sci. USA *108*, 1513–1518.

36. Simpson, J.T., Wong, K., Jackman, S.D., Schein, J.E., Jones, S.J.M., and Birol, I. (2009). ABySS: a parallel assembler for short read sequence data. Genome Res. *19*, 1117–1123.

37. Luo, R., Liu, B., Xie, Y., Li, Z., Huang, W., Yuan, J., He, G., Chen, Y., Pan, Q., Liu, Y., et al. (2012). SOAPdenovo2: an empirically improved memory-efficient short-read de novo assembler. Gigascience *1*, 18.

38. Altschul, S.F., Gish, W., Miller, W., Myers, E.W., and Lipman, D.J. (1990). Basic local alignment search tool. J. Mol. Biol. *215*, 403–410.

39. She, R., Chu, J.S.C., Wang, K., Pei, J., and Chen, N. (2009). GenBlastA: enabling BLAST to identify homologous gene sequences. Genome Res. *19*, 143–149.

40. Birney, E., Clamp, M., and Durbin, R. (2004). GeneWise and Genomewise. Genome Res. *14*, 988–995.

41. Edgar, R.C. (2004). MUSCLE: multiple sequence alignment with high accuracy and high throughput. Nucleic Acids Res. *32*, 1792–1797.

42. Martin, M. (2011). Cutadapt removes adapter sequences from high-throughput sequencing reads. EMBnet.journal *17*, 10–12.

43. Li, H., and Durbin, R. (2009). Fast and accurate short read alignment with Burrows-Wheeler transform. Bioinformatics *25*, 1754–1760.

44. Broad Institute (2019). Picard. http://broadinstitute.github.io/picard/.

45. Li, H., Handsaker, B., Wysoker, A., Fennell, T., Ruan, J., Homer, N., Marth, G., Abecasis, G., and Durbin, R.; 1000 Genome Project Data Processing Subgroup (2009). The Sequence Alignment/Map format and SAMtools. Bioinformatics *25*, 2078–2079.

46. Jónsson, H., Ginolhac, A., Schubert, M., Johnson, P.L., and Orlando, L. (2013). mapDamage2.0: fast approximate Bayesian estimates of ancient DNA damage parameters. Bioinformatics *29*, 1682–1684.

47. McKenna, A., Hanna, M., Banks, E., Sivachenko, A., Cibulskis, K., Kernytsky, A., Garimella, K., Altshuler, D., Gabriel, S., Daly, M., and DePristo, M.A. (2010). The Genome Analysis Toolkit: a MapReduce framework for analyzing next-generation DNA sequencing data. Genome Res. *20*, 1297–1303.

48. Sievers, F., Wilm, A., Dineen, D., Gibson, T.J., Karplus, K., Li, W., Lopez, R., McWilliam, H., Remmert, M., Söding, J., et al. (2011). Fast, scalable generation of high-quality protein multiple sequence alignments using Clustal Omega. Mol. Syst. Biol. *7*, 539.

49. Drummond, A.J., and Rambaut, A. (2007). BEAST: Bayesian evolutionary analysis by sampling trees. BMC Evol. Biol. *7*, 214.

50. Darriba, D., Taboada, G.L., Doallo, R., and Posada, D. (2012). jModelTest 2: more models, new heuristics and parallel computing. Nat. Methods *9*, 772.

51. GitHub (2015). Bam Util. https://github.com/statgen/bamUtil.

52. Nadachowska-Brzyska, K., Li, C., Smeds, L., Zhang, G., and Ellegren, H. (2015). Temporal dynamics of avian populations during pleistocene revealed by whole-genome sequences. Curr. Biol. *25*, 1375–1380.

53. Cingolani, P., Platts, A., Wang, L., Coon, M., Nguyen, T., Wang, L., Land, S.J., Lu, X., and Ruden, D.M. (2012). A program for annotating and predicting the effects of single nucleotide polymorphisms, SnpEff: SNPs in the genome of Drosophila melanogaster strain w1118; iso-2; iso-3. Fly (Austin) *6*, 80–92.

54. Purcell, S., Neale, B., Todd-Brown, K., Thomas, L., Ferreira, M.A.R., Bender, D., Maller, J., Sklar, P., de Bakker, P.I.W., Daly, M.J., and Sham, P.C. (2007). PLINK: a tool set for whole-genome association and population-based linkage analyses. Am. J. Hum. Genet. *81*, 559–575.

55. R Development Core Team (2017). R: A language and environment for statistical computing (Version 3.4. 2) (R Foundation for Statistical Computing).

56. Renaud, G., Slon, V., Duggan, A.T., and Kelso, J. (2015). Schmutzi: estimation of contamination and endogenous mitochondrial consensus calling for ancient DNA. Genome Biol. *16*, 224.

57. Schreiber, J. (2017). Pomegranate: fast and flexible probabilistic modeling in Python. J. Mach. Learn. Res. *18*, 1–6.

58. Faircloth, B.C., McCormack, J.E., Crawford, N.G., Harvey, M.G., Brumfield, R.T., and Glenn, T.C. (2012). Ultraconserved elements anchor thousands of genetic markers spanning multiple evolutionary timescales. Syst. Biol. *61*, 717–726.

59. Hoang, D.T., Chernomor, O., von Haeseler, A., Minh, B.Q., and Vinh, L.S. (2018). UFBoot2: improving the ultrafast bootstrap approximation. Mol. Biol. Evol. *35*, 518–522.

60. Kalyaanamoorthy, S., Minh, B.Q., Wong, T.K.F., von Haeseler, A., and Jermiin, L.S. (2017). ModelFinder: fast model selection for accurate phylogenetic estimates. Nat. Methods *14*, 587–589.

61. Nguyen, L.T., Schmidt, H.A., von Haeseler, A., and Minh, B.Q. (2015). IQ-TREE: a fast and effective stochastic algorithm for estimating maximum-likelihood phylogenies. Mol. Biol. Evol. *32*, 268–274.

62. Zhang, C., Rabiee, M., Sayyari, E., and Mirarab, S. (2018). ASTRAL-III: polynomial time species tree reconstruction from partially resolved gene trees. BMC Bioinformatics *19* (*Suppl 6*), 153.

63. Bouckaert, R., Vaughan, T.G., Barido-Sottani, J., Duchêne, S., Fourment, M., Gavryushkina, A., Heled, J., Jones, G., Kühnert, D., De Maio, N., et al. (2019). BEAST 2.5: An advanced software platform for Bayesian evolutionary analysis. PLoS Comput. Biol. *15*, e1006650.

64. Rambaut, A., Drummond, A.J., Xie, D., Baele, G., and Suchard, M.A. (2018). Posterior summarization in Bayesian phylogenetics using Tracer 1.7. Syst. Biol. *67*, 901–904.

65. Luther, D. (1986). Die ausgestorbenen Vögel der Welt, Fourth Edition (Westarp-Wissenschaften).

66. McKinley, D., and Hardy, J.W. (1985). The Carolina Parakeet in Florida (Florida Ornithological Society).

67. Allentoft, M.E., Sikora, M., Sjögren, K.G., Rasmussen, S., Rasmussen, M., Stenderup, J., Damgaard, P.B., Schroeder, H., Ahlström, T., Vinner, L., et al. (2015). Population genomics of Bronze Age Eurasia. Nature *522*, 167–172.

68. Dabney, J., Knapp, M., Glocke, I., Gansauge, M.T., Weihmann, A., Nickel, B., Valdiosera, C., García, N., Pääbo, S., Arsuaga, J.L., and Meyer, M. (2013). Complete mitochondrial genome sequence of a Middle Pleistocene cave bear reconstructed from ultrashort DNA fragments. Proc. Natl. Acad. Sci. USA *110*, 15758–15763.

69. Schubert, M., Ginolhac, A., Lindgreen, S., Thompson, J.F., Al-Rasheid, K.A., Willerslev, E., Krogh, A., and Orlando, L. (2012). Improving ancient DNA read mapping against modern reference genomes. BMC Genomics *13*, 178.

70. Bull, J.J. (1985). Sex determining mechanisms: an evolutionary perspective. Experientia *41*, 1285–1296.

71. Smith, C.A., Roeszler, K.N., Ohnesorg, T., Cummins, D.M., Farlie, P.G., Doran, T.J., and Sinclair, A.H. (2009). The avian Z-linked gene DMRT1 is required for male sex determination in the chicken. Nature *461*, 267–271.

72. Faircloth, B.C., McCormack, J.E., Crawford, N.G., Harvey, M.G., Brumfield, R.T., and Glenn, T.C. (2012). Ultraconserved elements anchor thousands of genetic markers spanning multiple evolutionary timescales. Syst. Biol. *61*, 717–726.

73. Miller, M.A., Pfeiffer, W, Schwartz, T. (2010). Creating the CIPRES Science Gateway for inference of large phylogenetic trees. Gateway Computing Environments Workshop (GCE) IEEE. https://www.phylo.org/sub_sections/portal/sc2010_paper.pdf.

74. Nabholz, B., Lanfear, R., and Fuchs, J. (2016). Body mass-corrected molecular rate for bird mitochondrial DNA. Mol. Ecol. *25*, 4438–4449.

75. Smeds, L., Qvarnström, A., and Ellegren, H. (2016). Direct estimate of the rate of germline mutation in a bird. Genome Res. *26*, 1211–1218.

STAR★METHODS

KEY RESOURCES TABLE

REAGENT or RESOURCE	SOURCE	IDENTIFIER
Biological Samples		
Conuropsis carolinensis tissue samples	Arboretum Masjoan private collection at Espinelves (Girona, Spain)	N/A
Aratinga solstitialis	Blood sample from *Aratinga* breeder	N/A
Deposited Data		
Whole genome data of one historical *Conuropsis carolinensis* sample	This paper	PRJEB33130
Aratinga solstitialis assembly	This paper	PRJEB33135
Aratinga solstitialis annotation data	This paper	PRJEB33153
Taeniopygia guttata 3.2.4 annotated proteins from Ensembl	N/A	Release 85
Gallus gallus 5.0 annotated proteins from Ensembl	N/A	Release 85
Whole-genome sequencing data of *Acanthisitta chloris*	[10]	NCBI Project ID: PRJNA212877
Whole-genome sequencing data of *Agapornis roseicollis*	[31]	NCBI Project ID: PRJNA355979
Whole-genome sequencing data of *Amazona aestiva*	[32]	NCBI Project ID: PRJNA294082
Whole-genome sequencing data of *Amazona collaria*	N/A	NCBI Project ID: PRJNA490036
Whole-genome sequencing data of *Amazona guildingii*	[28]	Ultraconserved Elements (UCEs) extracted from whole genome data
Whole-genome sequencing data of *Amazona vittata*	[33]	NCBI Project ID: PRJNA171587
Whole-genome sequencing data of *Ara macao*	[34]	NCBI Project ID: PRJNA175470
Whole-genome sequencing data of *Eolophus roseicapilla*	[28]	Ultraconserved Elements (UCEs) extracted from whole genome data
Whole-genome sequencing data of *Melopsittacus undulatus*	N/A	NCBI Project ID: PRJNA72527
Whole-genome sequencing data of *Nestor notabilis*	[10]	NCBI Project ID: PRJNA212900
Whole-genome sequencing data of *Probosciger aterrimus*	[28]	Ultraconserved Elements (UCEs) extracted from whole genome data
Whole-genome sequencing data of *Psittacula krameri*	N/A	NCBI Project ID: PRJNA377329
Targeted capture ultraconserved elements for *Conuropsis carolinensis*	This paper	N/A
Targeted capture ultraconserved elements for *Aratinga solstitialis*	This paper	N/A
Targeted capture ultraconserved elements for *Amazona autumnalis*, *Cacatua sulphurea*, *Psittacula alexandri*, *Psittacus erithacus*, *Strigops habroptila*	[21]	https://doi.org/10.5061/dryad.2vd01grFile: passerines.unaligned.uce.contigs.tar.gz
4,988 aligned UCE loci	This paper	https://doi.org/10.17632/ p4wt7jc9 dw.1
4,988 gene trees from UCE loci and summary tree from ASTRAL-III	This paper	https://doi.org/10.17632/ p4wt7jc9 dw.1
Concatenated dataset of 4,988 aligned UCE loci and resulting IQTREE tree	This paper	https://doi.org/10.17632/ p4wt7jc9 dw.1
Concatenated dataset of 2,755 aligned UCE loci which are present in 95% of taxa and resulting IQTREE tree	This paper	https://doi.org/10.17632/ p4wt7jc9 dw.1
Concatenated dataset of 893 aligned UCE loci which are present in 100% of taxa and resulting IQTREE tree	This paper	https://doi.org/10.17632/ p4wt7jc9 dw.1

(Continued on next page)

Continued

REAGENT or RESOURCE	SOURCE	IDENTIFIER
BEAST input files for 2 sets of 50 loci with calibration constraints and resulting trees	This paper	https://doi.org/10.17632/ p4wt7jc9 dw.1
Commands used for bioinformatic processing and phylogenetic analysis	N/A	https://doi.org/10.17632/ p4wt7jc9 dw.1
SOFTWARE AND ALGORITHMS		
ALLPATHS-LG	[35]	v.52485
AbySS	[36]	v.1.3.5
SOAPdenovo	[37]	v.2
TblastN	[38]	v.2.2.2
genBlastA	[39]	v.1.0.4
GeneWise	[40]	v.2.4.1
MUSCLE	[41]	v.3.8.31
cutadapt	[42]	v1.9.1
BWA	[43]	v.0.7.1
Picard	[44]	v2.0.1
Samtools	[45]	v.1.6
mapdamage2	[46]	2.7.12
GATK	[47]	3.7
ClustalOmega	[48]	1.2.1
BEAST	[49]	v.1.8.4 (v.2)
JmodelTest	[50]	v.2.1.10
BamUtil	[51]	v1.0.13
PSMC	[52]	v1.0
SNPeff	[53]	v4.3
PLINK	[54]	v1.9b
R	[55]	v3.5.1
SIFT	[14]	v6.2.1
Schmutzi	[56]	v1.5.4
Pomegranate	[57]	python v3
bcftools	N/A	v.1.9
PHYLUCE	[58]	v.1.6.6
IQTREE (incl. ModelFinder and UFBoot)	[59–61]	v.1.6.10
ASTRAL-III	[62]	v.5.6.3
BEAST2	[63]	v.2.6.0
Tracer	[64]	v.1.7

LEAD CONTACT AND MATERIALS AVAILABILITY

Further information and requests for resources and reagents should be directed to and will be fulfilled by the Lead Contact, Pere Gelabert (peregelabertx@gmail.com). This study did not generate new unique reagents.

EXPERIMENTAL MODEL AND SUBJECT DETAILS

Conuropsis carolinensis specimen

At least 720 skins and 16 Carolina parakeet skeletons are preserved in museum collections globally [65, 66]. We sampled one such specimen with the intention of generating the first near-complete whole genome information of the species. The specimen is preserved in a private collection in the village of Espinelves (Girona, Spain), and was collected at the beginning of the 20th century by the Catalan naturalist Marià Masferrer i Rierola (1856-1923).

The Carolina parakeet is believed to have consisted of two subspecies: *Conuropsis carolinensis carolinensis*, that was principally distributed in Florida and along the Southeast coast of United States, and *Conuropsis carolinensis ludovicianus* that was distributed

across the central states of the country [2]. Both subspecies could be differentiated by morphological features such as coloration and body size. The wing, bill, and tail lengths of all adult *C. c. ludovicianus* significantly averaged more than in all adult *C. c. carolinensis* [4]. The wing and tarsal lengths (Figure S1), as well as the general color pattern of the Espinelves specimen, indicate it belongs to *C. c. carolinensis*.

Aratinga solstitialis specimen
A sample of blood was obtained *in vivo* from a female specimen from an official *Aratinga* breeder.

METHOD DETAILS

Conuropsis DNA extraction and sequencing
Two different samples of about 100 mg were obtained, one from the femur (leg bones were preserved inside the naturalized specimen) and one from toepads, with the help of a Dremel machine.

The two samples were digested using 2mL of extraction buffer containing 10mM Tris-HCL (pH 8), 10mM NaCl, 5mM $CaCl_2$, 2.5mM EDTA, 1% SDS, 1% Proteinase K and 40mM DTT. The solution was resuspended by vortexing and was incubated in a rotating plate overnight at 55°C. Digested samples were purified, and DNA was isolated following a combination of Phenol/Chloroform and column purification, as outlined below.

After incubation, digested samples were centrifuged for 3 min at 3000 × g and the supernatant was collected and mixed with 1X volume of Phenol. The sample solution was incubated on a rotor for 5min at RT. After, it was centrifuged for 3 min at 5000 × g and the upper aqueous layer was collected in new low-bind Eppendorf tube. The collected aqueous layer was mixed with 1X volume of Chloroform and the process was repeated. Again, the upper aqueous layer was collected in new tube and mixed with 10X volume of binding buffer prepared as previously described [67].The sample solution mixed with the binding buffer was poured into a binding apparatus constructed by fitting an ZymoV extension reservoir in a MinElute column and set inside a 50mL Falcon tube (as in [68]. Samples were centrifuged at 300 × g until all the liquid had passed through. The MinElute column was then separated from the reservoir and set into a new 2ml low-bind collection tube. The column was washed with 730μL of QIAGEN buffer PE, centrifuged at 3,300 × g, flow-though was discarded and the MinElute column was dry-spun for 1 min at 6000 × g in a bench-top centrifuge. DNA was eluted in a final volume of 50μL by adding twice 25μL of QIAGEN EB buffer and incubating for 5 min at 37°C between each elution. Samples were centrifuged at 6000 × g and extracted DNA was quantified using a Qubit instrument.

Following extraction, 15 μL of DNA extract was built into blunt-end libraries using both the NEBNext DNA Sample Prep Master Mix Set 2 (Cat No. E6070) and the BEST protocol using BGI adapters (as in [11]. Two libraries were built for each method. For the NEB protocol, the libraries were prepared according to manufacturer's instructions, only skipping the initial nebulization step.

The resulting DNA library for each method was then amplified and indexed in 4 PCR reactions of 50μL each with 16μL of DNA template on each, mixed with 25 μL 2X KAPA U+ Buffer, 1.5 μL of BGI amplification primer (10 μM)(sequences described in [11]. Thermocycling conditions were 3 min at 98°C, followed by 22 cycles of 20 s at 98°C, 30 s at 60°C and 30 s at 72°C, and a final 7 min elongation step at 72°C. The amplified library was purified with PB buffer on QIAGEN MinElute columns, before being eluted in 30 μL EB. Negative library controls, constructed with H_2O, were included, as well as libraries constructed on the negative extraction controls; both subsequently yielded no DNA sequences.

Amplified libraries were quantified using a TapeStation instrument (Agilent) and two sequencing pools were created by merging the amplified libraries for each method and sequenced on 2 lanes of a BGISEQ-500 sequencing instrument using 100SR chemistry. Libraries prepared from tibia bone powder exhibited longer DNA reads in comparison with the toe tissue (x = 83bp versus x = 61 bp, p < 0.001). NEB libraries yielded longer DNA reads than BEST libraries (x = 84.86 and x = 63.45 versus x = 75.39 and x = 60.31 in tibia and toe respectively, p < 0.001). NEB libraries were also the ones that yielded higher endogenous DNA content as well as lower clonality.

Aratinga solstitialis DNA extraction
Parallel genomic DNA extractions were performed on blood from a single *Aratinga solstitialis* female individual using the DNeasy Blood & Tissue Kit (QIAGEN, Valencia, CA) following manufacturer's instructions. The resulting DNA extracts were quantified using the Qubit 2.0 Fluorometer (Thermo Fisher Scientific, Waltham, MA) with no modification of its standard protocol. To check for molecular integrity, each DNA extract was run on the 2200 TapeStation (Agilent Technologies, Santa Clara, CA) following manufacturer's protocol.

Aratinga solstitialis sequencing and assembly
Using the high molecular weight (HMW) DNA extracts, a short PCR-free insert library with 180 bp inserts was prepared using TruSeq DNA kit (Illumina, CA, USA) according to the manufacturer's instructions. In addition, three different mate-pair libraries were built using the Nextera protocol (Illumina, CA, USA). These comprised one 3 kb mate-pair library, one 5 kb mate-pair library, and one 20kb mate-pair library. All libraries were indexed to enable de-multiplexing after sequencing. The libraries were subsequently sequenced on the Illumina HiSeq X platform (using 2 × 150 bp reads), where the first lane was used for the 180 bp insert library. For the second lane, the three mate-pair libraries were pooled in equimolar ratios prior to sequencing.

In order to generate a *de novo* assembly, three different assemblers were used: ALLPATHS-LG v.52485, ABySS v.1.3.5 and SOAPdenovo. Out of the three assemblers, ALLPATHS-LG gave the best result, with an N50 scaffold measure of 19.5Mbp.

Aratinga solstitialis annotation

We used a homology-based method to annotate the protein-coding genes in the *Aratinga* genomes by using Ensembl gene sets (release 85) of chicken (*Gallus gallus*), zebra finch (*Taeniopygia guttata*) and human (*Homo sapiens*), and genes derived from published avian transcriptomes. The protein sequences of the reference gene set compiled above were used as references for homology-based gene prediction.

We aligned reference protein sequences to the genome by TBLASTN with an E-value cut-off of 1e-5. We linked the hits into candidate gene loci with genBlastA and removed candidate loci with a homologous block length shorter than 30% of length of query protein. We extracted genomic sequences of candidate gene loci and 2,000bp upstream/downstream sequences as input for GeneWise to predict gene models in the genome. Then we translated the predicted coding regions into protein sequences, and ran MUSCLE for each pair of predicted protein and reference protein. We filtered out the predicted proteins with length of < 30aa or percent identity < 40%, as well as the pseudogenes (genes containing > 2 frameshifts or pre-mature stop codons) and retrogenes. The output of GeneWise could include redundant gene models, which overlap at the same genome regions. Hierarchical clustering was applied to the output of GeneWise to build a non-redundant gene set. Genes that overlapped in > 40% of their coding sequence were clustered and kept the sequence with the highest identity to the reference genes. We removed the highly duplicated genes (frequency of duplications > 10) in two conditions: 1) with a single exon; 2) with > 70% repeat sequences in coding region.

Conuropsis carolinensis mapping and variant calling

The ancient DNA reads were clipped using cutadapt; sequencing adapters were removed. Only reads longer than 30bp were kept. Filtered reads were mapped against the *A. solstitialis* assembly with Burrows-Wheeler Aligner (BWA) [69], setting no trimming, disabling seed, increasing stringency for edit distance, and allowing opening of 2 gaps. Duplicated reads were removed using Picard-tools MarkDuplicates. Mapped reads with mapping quality below 30 were removed using Samtools. The resulting reads were examined with mapdamage2 to assess the degradation rate of the data, which is a sign of authenticity. We detected the presence of typical aDNA-damaged bases at the end of reads. To avoid problems in the next steps, we trimmed 2 nt from each read end using BamUtil trimbam.

Genotypes were estimated using GATK UnifiedGenotyper. We removed calls with base quality below 30 (-mbq), and we set the rest of parameters as default. The average depth of coverage of the sample was 13.4X. To prevent variant calling errors in repetitive or complex regions, we used GATK SelectVariants to exclude the calls with depths of coverage below 10x and above 35X. Afterward we also used GATK SelectVariants and GATK FilterVariants to exclude from the call-set InDels and heterozygous calls in allele frequencies below 0.2 and above 0.8. We subsequently used the *A. solstitialis* assembly annotations to build a SNPeff database and used *Gallus* annotations to determine derived alleles.

Sex determination

The *Aratinga* genome -which we knew was a female- showed, as expected, half of coverage in the ZW chromosomes [70]. We plotted the depth of coverage distribution for each scaffold of the Carolina parakeet using Samtools and found identical coverage distribution. We subsequently searched for the *DMRT1* gene [71] to confirm the *Aratinga* Z chromosome scaffold.

Ultraconserved Elements (UCE) phylogenetic tree

For phylogenetic analysis, we targeted 5,060 UCE loci from 14 species with whole genome sequences (including the two new genomes presented here) and from 5 parrots that were included in a previous UCE capture study [21]. The Tetrapods-UCE-5Kv1 bait set [72] was applied to 18 parrots and the outgroup *Acanthisitta chloris*. A total of 4,988 UCE sequences were identified and extracted with the flanking 1000bp to both sides, aligned and trimmed using PHYLUCE (commands in 10.17632/p4wt7jc9dw.1). *Strigops habroptila* from the targeted capture study had significantly fewer and shorter loci than all other samples (1,648 loci, 269bp length on average compared to 757bp on average across samples from [21]) but we kept the sample because of its significance for fossil calibration.

We used coalescent and concatenation approaches to infer phylogenetic relationships. First, we constructed maximum likelihood gene trees for all 4988 alignments using IQTREE with 1000 ultrafast bootstrap replicates after determining the most appropriate nucleotide substitution model with ModelFinder. The resulting gene trees were summarized into a coalescence-based species tree using ASTRAL-III. Second, we concatenated all loci (9,864,148bp), the 2,755 loci that were present in 95% of all species (5,561,275bp) and the 893 loci that were present in 100% species (1,840,245bp) and analyzed them as above.

For calibration analyses, we drew two random samples of 50 loci that had all taxa and had the same substitution model (HKY+F+G4, the most common model across all loci). For both random samples, we executed two MCMC chains (100 million generations, sampled every 5,000 generations) in BEAST2 on the CIPRES Science Gateway [73]. Each analysis was performed on the topology from concatenation, employing a birth-death model, a relaxed clock model with lognormal distribution on the rate prior and HKY+F+G4 as the substitution model. The age of two nodes was constrained with lognormal distributions following the thorough published fossil justifications [21]. First, a lognormal prior was placed on the root of the tree (Passeriformes+Psittaciformes, *Eozygodactylus americanus*) with an offset of 51.81 Mya and a 97.5% quantile encompassing 66.5 Mya. Second, a lognormal prior was placed on

the MRCA of *Strigops+Nestor* (*Nelepsittacus minimus*) with an offset of 15.9 Mya and a 97.5% quantile at 66.5 Mya. Replicate runs were checked for convergence in Tracer, combined and annotated after a burning of 30% with LogCombiner and TreeAnnotator.

Mitochondrial phylogenetic tree

Trimmed DNA reads (209,887,920) were mapped against *A. solstitialis* mtDNA genome (JX441869). The mtDNA consensus sequence of *Conuropsis* was obtained by using schmutzi endoCaller and aligned with Clustal Omega to 11 other Arini mtDNA genomes and *Amazona ventralis* as outgroup. The obtained alignment of 13 sequences of 18,731bp in total length was dated using BEAST based on a fixed clock rate of 0.0042 substitutions/site/MY for all coding regions, which was previously determined for the brown-throated Parakeet *Eupsittula (*formerly *Aratinga) pertinax* [74]. The number of polymorphic sites of *Conuropsis* mtDNA genome in the alignment was 4,369. We used the GTR+I+G nucleotide substitution model selected by jModelTest with the Akaike Information Criterion.

Conuropsis population history

We used the Pairwise Sequentially Markovian Coalescent (PSMC) model to explore the demographic history of *C. carolinensis*. We obtained a fastq sequence of *C. carolinensis* for autosomal regions in scaffolds longer than 100Kbps. Only positions with a depth of coverage above 8X and below 50X were kept. Posteriorly a PSMC was built using the following parameters: -N25, -t15, -r5, -p "4+25*2+4+6." We used age of sexual maturity (1 year) [3], multiplied by a factor of two as a proxy for generation time, following the same approach as in a previous study of PSMC in 38 avian species [52] and a mutation rate of 2.3×10^{-9}, estimated from bird pedigree information [75].

Conuropsis average genome heterozygosity

To identify regions of the *C. carolinensis* genome that shows signs of homozygosity we plotted the distribution of heterozygous positions across the genome sequence. We examined the scaffolds counting the number of heterozygous positions in windows of 50Kb with 10Kb of overlap. We define the average genome heterozygosity as the proportion of heterozygous sites genome-wide divided by the total number of callable bases. We kept only SNV sites applying the following filtering criteria: Read Depth > 10, Genotype Quality > 20, Allele Balance 0.2 < AB < 0.8 (hypergeometric distribution 0.95 CI [0.233-0.766]). All variable repeats, indels and multiallelic sites were removed. Non-variable sites were considered callable if their read depth was larger than 10. Additional heterozygosity values for other bird species were extracted from published avian genomes [10].

Conuropsis Runs of Homozygosity (RoHs)

RoHs were called based on the density of heterozygous sites in the genome using a Hidden Markov Model (HMM) for segmentation: First, the *Aratinga* reference genome was partitioned into 50Kb windows guided by the *Conuropsis* callability mask, namely, uncallable *Conuropsis* sites were omitted in the window tally. Heterozygosity values were calculated for each window as described above. Next, an HMM (python3 pomegrenate package) was fitted to the data. Emissions were modeled based on the empirical window heterozygosity distribution with a two/three component Gaussian Mixture Model (GMM). The first component of the GMM was reserved to extremely small heterozygosity values in order to capture the RoH variability, while the second component was allowed to vary freely. If necessary, a third mixture component was added to capture outliers. The transition probabilities were trained using the Baum-Welch algorithm.

QUANTIFICATION AND STATISTICAL ANALYSIS

All statistical details of experiments can be found at the STAR Methods. The phylogenetic tree in Figure 1 was performed with BEAST 2 (https://www.beast2.org). The pattern of post-mortem damage in Figure S1 was generated with mapdamage2 and the contamination estimates at the mtDNA was done with Schmutzi program. Adaptors from the DNA reads were removed with cutadapt. Genetic differences between *Conuropsis* and *Aratinga* were explored with SIFT software and the prediction of effects of some polymorphisms was done with SNPeff software.

DATA AND CODE AVAILABILITY

The accession numbers for the *Conuropsis* and *Aratinga* genomes reported in this paper are in the European Nucleotide Archive (ENA): PRJEB33130 and PRJEB33153, respectively.